# Finger-Adaptive Illumination Control and Exposure Fusion Imaging for Biometric Finger Vein Recognition

Perera, R. A. H.
University of Twente
P.O. Box 217, 7500AE Enschede
The Netherlands
r.a.h.perera@student.utwente.nl

## ABSTRACT

Finger vein recognition is an emerging technique in biometrics. Capture of sufficient vein detail from a well-exposed image is crucial for its operation. We present a novel finger-adaptive illumination control algorithm and an exposure fusion based imaging procedure for finger vein imaging on a prototype device. The novel approach enables sub-second capturing of well-exposed images and shows significant improvements in match scores.

## Keywords

Biometrics, Finger Vein Recognition, Adaptive Illumination, Exposure Fusion

## 1. INTRODUCTION

Biometrics is the science of establishing the identity of an individual based on the physical, chemical or behavioral attributes of the person [6]. Fingerprint, face, and iris recognition are currently widely used. Patterns of veins beneath the skin on fingers can also be used for this purpose. This mode of biometric recognition is characterised by very low error rates, good spoofing resistance, and a user convenience similar to that of fingerprint recognition [15].

The Data Management and Biometrics (DMB) group at the University of Twente has developed a prototype device[1] to further study finger vein recognition [14, 12]. The accuracy of the authentication is heavily reliant on the quality of the captured images and the visibility of vein patterns therein. We present a novel finger-adaptive illumination algorithm that does not require manual tuning once calibrated per-device, and an approach to obtain better vein images via exposure fusion. The novel methods enable finger vein image capture in less than a second, while being robust to finger thickness variations.

The paper starts with a brief background about the device, issues regarding illumination and image capture, as well as current solutions to the problems. We then condense the issues that this research addresses into research questions. Thereafter, we briefly present the state of the art on the topic. We then present the main body of the research as well as its evaluation using a preliminary study.

[1]see Figure 5 in Appendix B


*31$^{st}$ Twente Student Conference on IT* Jul. 5$^{th}$, 2019, Enschede, The Netherlands.


## 2. BACKGROUND

The device functions by illuminating a finger with infrared (IR) light with an array of IR LED's and capturing an image of the finger using a camera placed behind an IR filter. Each LED in the array can be individually controlled via pulse width modulation (PWM), which is essentially specifying a fraction of the time a given LED can stay on in single clock cycle.

IR light at the wavelength used by the device can penetrate skin, muscle, and bone tissue to different extents, but is heavily absorbed by haemoglobin in blood vessels. Hence, the blood vessels (hereinafter called veins for simplicity) under the skin are visible in these captures as dark lines. These captured images can then be compared with those in a database of prior captures to authenticate.

As introduced before, vein visibility in images is crucial for the comparison procedure. Illumination is critical to obtain more vein visibility, by preventing the saturation of the camera. Too much light can saturate the camera, and too little will not be sufficient to penetrate the finger. The level of illumination required differs both along a finger and across fingers, due to differences in physiology. For instance, joints cause very little NIR light loss compared to bones.

A method was devised by Jin [7] to obtain uniform illumination along a finger, in order to solve this issue. However, this algorithm is iterative, and does not always converge. In addition, it may take in the order of seconds to terminate, making it cumbersome to use. Even then, obtaining perfectly uniform illumination appeared to be difficult.

Due to the aforementioned drawbacks, a novel approach had been developed to increase the quality by obtaining multiple images at different illumination levels and combining them to form a High Dynamic Range (HDR) image [5, 16]. However, the new HDR approach also has room for improvement with respect to adaptive illumination in order to be robust against finger thickness variations, as well as the quality of the final image and acquisition time. The illumination needs to be manually tuned per finger. The HDR generation takes about 15 images per finger as input, making the capturing and processing time high. The long acquisition time also introduces motion blur due to movements of the finger in this duration.

Thus, a combined approach which provides both finger-adaptive illumination as well as obtains images in a time efficient manner with sufficient quality is needed.

# 3. RESEARCH QUESTIONS

Accordingly, the research aims to address the following research questions.

**RQ1** How can a linear array of LEDs be controlled such that the light passing through a finger placed under them is as uniform along its length as possible as well as of the right amount to prevent camera saturation, without needing feedback iterations?

**RQ2** How can an alternative finger vein imaging procedure to that described by Humblot-Renaux [5] be composed to incorporate an illumination control algorithm that is described by RQ1 to form an imaging pipeline that provides enhanced images with a fewer number of captures?

**RQ3** To what extent does the accuracy of finger vein image comparison improve, with the solutions in RQ1 and RQ2, where accuracy is measured by the scores of the maximum curvature method developed by Miura et al [10]?

# 4. RELATED WORK

## 4.1 Adaptive Illumination

Related work is scarce for adaptive illumination of this nature. Nonetheless, Jin's work [7] establishes that it is indeed possible to control LEDs individually in order achieve a more uniform illumination as opposed to controlling the entire array as a whole. Another research by Chen *et al.* [3] uses a method similar to that by Jin, however, this algorithm too is iterative and is subject to the same limitations.

Work by Debevec and Malik [4] on radiance map estimation is also of relevance to this research. Their work establishes that the camera's output and actual radiance in a scence are roughly logarithmic unless saturated. This fact is also used by Chen *et al.* [3] in their algorithm and is relevant to controlling illumination.

## 4.2 Improvement of Image Capture

Sa, Carvalho, and Velho [13] have compiled a collection of general approaches to HDR image generation from LDR images. They aim to estimate the camera's intensity response function, and thereby infer the actual radiance of individual pixels in the captured image to accurately reconstruct a HDR image.

Vissers [16] and Humblot-Renaux [5] have seen success at using an HDR approach to finger vein acquisition. The work of Humblot-Renaux is the most recent. Humblot-Renaux uses weighted sum of the LDR images, where the weights are the background illumination levels of a region, estimated by a mean filter. Further, Piciucco *et al.* [11] have tried a similar approach to palm vein image acquisition, and also analysed the performance of various tone mapping functions.

An alternative approach to HDR imaging is to fuse well-exposed regions of multiple exposures to obtain a globally well-exposed image. Mertens *et al.* [9] provides a novel approach for this purpose for general purpose images. The image is decomposed into a 'pyramid' structure based on measures for contrast, saturation, and exposure, and then fused together with a given weight for each of the three factors. This approach avoids the need for a high dynamic range image and a tone mapping intermediate step to generate high quality images.

Chen *et al.* [2] have presented a multiple image fusion method for finger vein images and shows promising results. However, their approach fuses vertical 'stripes' of multiple images together instead of a more general pyramid decomposition approach, which is also robust against vertical variations in exposure. Chen's method also does not take into account local contrast and saturation, while that by Mertens does.

# 5. METHODOLOGY AND APPROACH

## 5.1 Adaptive illumination

The developed finger-adaptive feed-forward illumination algorithm provides a 'best effort' level of uniform illumination. The high-level steps in the algorithm are as follows.

1. Initial calibration to estimate camera response parameters and light distribution of each LED.
2. Measurement of light loss along the finger using an image captured at a constant, uniform, known illumination level.
3. Illumination adjustment based on calibration and measurement data.

Step 1 has to be carried out only once per device, unless its structure or camera parameters change. In the reference implementation, this is done at device startup. Steps 2 and 3 have to be carried out per finger (prior to capture). This procedure could also be carried out once per finger and stored together with its enrolled image for re-use during authentication.

### 5.1.1 Model

We model a finger as a translucent medium which loses a portion of NIR light falling on it (due to reflection, absorption and scattering) while letting the rest pass through. The proportion of light passed through varies at different points in the finger. Prior research shows that the global variation of this proportion along the finger is primarily along its length due to bone-joint structure, while local variations are primarily due to blood vessels. Hence, we simplify the finger as a thin line along which the proportion of light loss varies, where the loss proportion is the average of those at that horizontal position. The directions and coordinate system used are illustrated in Figure 6 of Appendix B.

The LED array is modelled as source of light of which each LED is identical and has a light output that is directly proportional to its PWM fraction. This is reasonable since PWM control simply controls the duration for which the light stays on, and hence provides output proportional to the fraction provided. The LED array is simplified as a thin line aligned with the finger along which luminous intensity can be varied. We also assume that the incident light intensity at a certain position along the finger is strongly correlated with the light exiting the finger at a position directly below, subject to loss.

We model the camera as a sensor of which the output at a given position is proportional to integral incident light intensity at the position over time, given that it is not close to saturation. This model is based in the work by Debevec and Malik. [4]

Now, if we can estimate

1. the parameters of the logarithmic function for camera output which relates light intensity to camera output,

2. the distribution of light output of each LED as incident on the finger, and
3. the proportion of light loss at each position along the finger,

we can also, given a required uniform luminous intensity along a finger,

4. use the finger loss proportions and determine the required distribution of luminous intensity along its length to compensate for loss, and
5. estimate the required light intensities of the different LEDs to approximate in the required compensatory luminous intensity distribution at the top of the finger.

Thus, we now have a simplified model which we can use to address **RQ1**.

### 5.1.2 Device calibration

In order to address steps 1 and 2 of the simplified model, a calibration procedure is required. The proposed calibration procedure is as follows.

1. Insert a thin, uniform diffuser such as a piece of 80 gsm white paper covering the finger slot.
   *This ensures that the focused light output of the LEDs are diffused sufficiently for the camera to capture.*
2. Iterate linearly through PWM fractions of an LED in the middle, starting from 0.125 and incrementing in steps of 0.125, and capture these images.
   *We assume here that the light output from each LED is approximately the same, and thus only one LED is required.*
3. Determine the average vertical gray levels within the capture window for each horizontal position and determine the maximum value for each capture.
   *This step is to fit the modelling of the LED array as a thin, linear light source and detect a single peak value that can be used to determine the logarithmic relation.*
4. Run logarithmic regression with PWM values as the independent variable and gray levels as the dependent variable. Store the constants $a$ and $b$ such that $gray\_level = a + b \cdot \log(pwm)$. These values correspond to the data required in step 1 of the refined problem model.
5. Iterate through all LEDs at maximum PWM (1.0) and determine the average vertical gray levels for each horizontal position for each LED image. Add these values to a matrix $\mathbf{G}$ where the $i^{\text{th}}$ row contains average gray level distribution of the $i^{\text{th}}$ LED. That is, if $\mathbf{I}^i$ is the image $W \times H$ (i.e. an $H \times W$ matrix) obtained with only the $i^{\text{th}}$ LED on at a 1.0 PWM fraction,

$$\mathbf{G}_{ij} = \frac{\sum_{k=1}^{H}(I^i_{kj})}{H}.$$

   *This step is to determine the light distributions due to each LED in the array along the modelled line.*
6. Transform $\mathbf{G}$ by $\mathbf{L} = e^{\frac{\mathbf{G}-a}{b}}$ element-wise. The values in $\mathbf{L}$ are now those required in step 2 of the refined problem model.

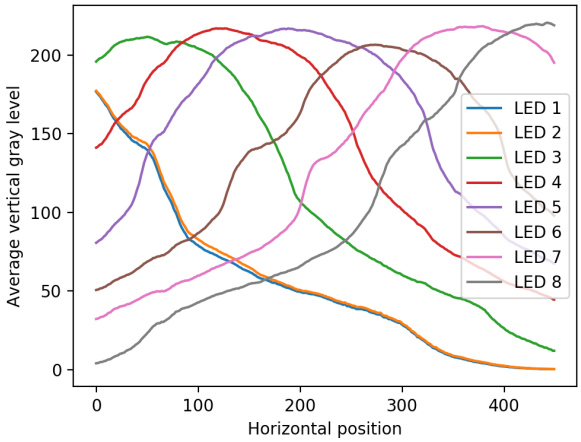


**Figure 1. Plots of average gray levels due to LEDs. Each line corresponds to a row in G.**

*This step transforms the sensed levels by inverting them using estimated the camera function to be able to linearly combine light intensity distributions of the LEDs to obtain the total incident light intensity at the finger at different PWM fractions.*

The transformed values $\mathbf{L}$ in are now directly proportional to actual incident light intensities along the length of the finger due to each LED.

### 5.1.3 Finger measurement

The next procedure addresses step 3 in the process.

1. Set PWM values to 1.0.
2. Take image of finger, crop, and apply finger mask[2]. Let the masked image of the finger be $\mathbf{M}$.
3. Transform each value $v$ in the image by $\mathbf{v}' = e^{\frac{\mathbf{v}-a}{b}}$.
   *This step transforms the sensed gray levels by the inverse of the estimated camera function to obtain values that can be linearly manipulated.*
4. Calculate the average gray values across the width of the finger (for each position along its length), and let this be a vector $\mathbf{f}$. Formally, if $H$ is the height of the image and $H^f_j$ is the finger thickness at position $j$ along its length, then

$$\mathbf{f}_j = \frac{\sum_{i=1}^{H}\mathbf{M}_{ij}}{H^f_j}$$

   *This to fit the simplified linear model of the finger.*
5. Take the column sum of $\mathbf{L}$ and let this be $\mathbf{s}$. Divide $\mathbf{f}$ by $\mathbf{s}$ element-wise to obtain the finger constants $\mathbf{k}$.

Since the values in rows of $\mathbf{L}$ are directly proportional to the light intensity distribution of the LEDs, its column sum $\mathbf{s}$ is directly proportional to the total incident light intensity distribution on the finger. Further, $\mathbf{f}$ contains the light intensity distribution along the finger with losses. Therefore, $\mathbf{k} = \frac{\mathbf{f}}{\mathbf{s}}$ now contains the constants of proportionality which relate the light intensities obtained during calibration and those observed via the finger with loss.

[2] will be outlined later in the text

### 5.1.4 Illumination adjustment

Having obtained the requisite data from device calibration and finger measurement, we can now proceed to address step 4 of the refined problem model.

1. If the desired uniform gray level along the finger is $u$, determine the appropriate light distribution $\mathbf{c}'$ to compensate for loss by taking $\mathbf{c}' = \mathbf{1.0} \times e^{\frac{u-a}{b}}$. Here, $\mathbf{1.0}$ is a row vector of length $W$ (image width) containing the value 1.0.
2. Sanitize $\mathbf{c}'$ to $\mathbf{c}'$ obtain such that $\mathbf{0} \leq \mathbf{c} \leq \mathbf{s}$ element-wise.

$$\mathbf{c}_i = \begin{cases} \mathbf{s}_i & \mathbf{s}_i < \mathbf{c}'_i \\ \mathbf{c}'_i & 0 \leq \mathbf{c}'_i \leq \mathbf{s}_i \\ 0 & \mathbf{c}'_i < 0 \end{cases}$$

*This is since the luminous intensities can never exceed those at max PWM of all LEDs.*

What remains is step 5, the last and most significant step. The goal here is to find the intensity fractions of each LED such that the sum of their horizontal intensity distributions result in the desired horizontal light intensity distribution.

We already have $\mathbf{L}$, a matrix whose $i^{\text{th}}$ row, $\mathbf{L}_{i*}$, consists values directly proportional to the average luminous intensity in the horizontal direction with only the $i^{\text{th}}$ LED on. Thus, $\mathbf{L}_{i*}$ contains the horizontal light intensity distribution at maximum intensity due to the $i^{\text{th}}$ LED. $\mathbf{c}$ is a row vector with the desired horizontal light intensity distribution. The problem can be refined as finding a row vector $\mathbf{p}$ such that

$$\mathbf{p} \times \mathbf{L} = \mathbf{c} \tag{1}$$

where $\mathbf{p}_i$ is the intensity fraction of the $i^{\text{th}}$ LED. At first glance, it may seem that determining a suitable (pseudo) right inverse of $\mathbf{L}$ would provide a solution. However, the range of values in $\mathbf{p}$ should be in the range $[0, 1]$, and no trivial generalized algorithm exists for such a problem. Hence, we propose to solve the problem using a simplified inverse multivariate regression algorithm which aims to find the closest approximation for $\mathbf{p}$. $\mathbf{L}$ and $\mathbf{c}$ together form the input to the regression algorithm.

We start with an initial approximation of $\mathbf{p} = \mathbf{1.0}$. Since $\mathbf{p}$ is an approximation, then the resulting horizontal light distribution row vector $\mathbf{v}$ may not be equal to $\mathbf{a}$. Formally, this is:

$$\mathbf{p} \times \mathbf{L} = \mathbf{v} \tag{2}$$

and

$$\mathbf{v} - \mathbf{c} = \mathbf{e} \neq \mathbf{0} \tag{3}$$

where $\mathbf{e}$ is the row vector of errors in the approximated horizontal light distribution. Now the goal of the regression is to minimise $\mathbf{e}$.

In order to determine the compensation be applied to each value in $\mathbf{p}$, it is necessary to find the contribution of each value in $\mathbf{p}$ to those in $\mathbf{e}$. For this purpose we define a weight matrix $\mathbf{W}$ which satisfies the following relation:

$$\mathbf{e} \times \mathbf{W} = \mathbf{d} \tag{4}$$

where $\mathbf{d}$ a column vector equal in size to $\mathbf{p}$, which gives the error contribution from each LED. We obtain the $\mathbf{W}$ as follows. Let the column sum of $\mathbf{L}$ be the row vector $s$.

$$\mathbf{s}_j = \text{sum}(\mathbf{L}_* j) \tag{5}$$

First we normalize each column of $\mathbf{L}$ by diving each row element-wise by $s$ to obtain $\mathbf{L}'$.

$$\mathbf{L}'_i* = \frac{\mathbf{L}_i*}{s} \tag{6}$$

Now each $\mathbf{L}'_{ij}$ contains the fraction of light intensity contribution from the $i^{\text{th}}$ LED to the $j^{\text{th}}$ horizontal position. We then scale each row in $\mathbf{L}'$ by the ratio between the original row's maximum and the maximum of the original matrix to obtain $\mathbf{L}''$.

$$\mathbf{L}''_i* = \mathbf{L}'_{i*} * \frac{\max(\mathbf{L}_{i*})}{\max(\mathbf{L})} \tag{7}$$

This is so that the relative magnitude of the LEDs remain constant despite the column normalisation. Finally, $\mathbf{W}$ is constructed as $\mathbf{L}''^T$ so as to fit the shape required for the matrix multiplication in Equation 4.

Finally, we can adjust the error values in $\mathbf{e}$ by dividing by $\mathbf{s}$, so that the values obtained in $\mathbf{d}$ are roughly on the same order of magnitude as the values in $\mathbf{p}$. $\mathbf{d}$ can then be used to adjust $\mathbf{p}$ by the following recurrence relation in each iteration of the regression algorithm:

$$\mathbf{p}_{k+1} = \mathbf{p}_k - \mathbf{d}_k. \tag{8}$$

The values of $\mathbf{p}$ can clamped to be in the range $[0, 1]$ since the LEDs can neither exceed the maximum intensity nor have negative intensities.

This process is then carried out for a constant maximum number of iterations (500 in reference implementation) or until the change in $\mathbf{p}$ in an iteration is significantly low ($< 10^{-4}$ in reference implementation). The regression algorithm is summarised as pseudo-code in Algorithm 1 in Appendix A.

## 5.2 Improvement of imaging

The next portion of the research deals answering **RQ2**. That is, how to obtain a high quality image that is suitable for vein pattern extraction using the adaptive illumination algorithm. We present an simpler alternative method to obtain a high quality vein image without going through the intermediate steps of high dynamic range imaging and tone mapping, namely *exposure fusion*.

Our method uses the exposure fusion algorithm by Mertens *et al.* [9] to compose an end-to-end illumination control, imaging, and pattern extraction pipeline that requires no manual adjustment beyond initial calibration. The algorithm also takes local contrast into account in addition to good exposure, which is of importance for vein images, since improved local contrast usually leads to better vein visibility. The pipeline is composed of the following high-level steps:

1. Image capture
2. Finger normalization and segmentation
3. Exposure fusion
4. Pattern extraction

### 5.2.1 Image capture

The image capture process takes several images at different constant, horizontally 'uniform' gray levels by making use of the procedure outlined in Section 5.1 above. The reference implementation uses four gray levels in the neighbourhood of 130, [120, 140, 160, 180] which has a reasonable level of brightness for human visual comparison while avoiding over or under exposure.

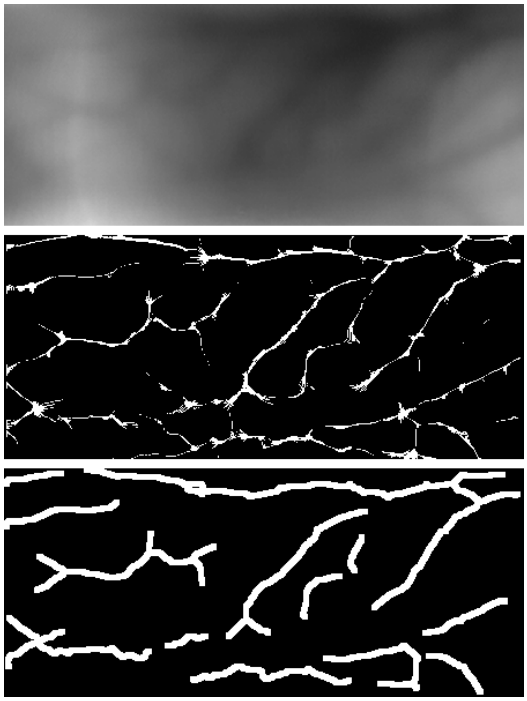

**Figure 2. The vein pattern extraction process. From top to bottom: raw vein image, pattern extracted using the maximum curvature method, enhanced pattern**

### 5.2.2 Finger normalization and segmentation

The finger images captured should then be normalized and segmented to obtain a region of interest containing finger veins for the pattern extraction process.

Our proposed method starts by detecting candidates for finger edges using Canny edge detection [1]. The detected edges are then ranked based on length and the longest edges in the top and bottom half of the image are chosen as the pair of finger edges. The edges are then extended to reach the right and left edges of the image and combined to form a finger contour. This contour is then used for creating the finger mask. This method was found to be more robust against non-finger artifacts in the image due to reflections from parts of the imaging device than the method proposed by Lee *et al.* [8].

We use the detected edges to determine a midline of the finger by fitting a line to the average of the vertical positions of the two edges, for each horizontal position. The normalisation process applies a transformation matrix derived from the gradient and intercept of the midline in order to compensate for the rotational and translational deviations in finger position. The same is performed for the derived mask to form a mask that matches the transformed image.

The final step applies the mask to the image to provide a normalized and segmented finger image.

### 5.2.3 Exposure fusion

The exposure fusion process receives the normalized multi-exposure images and combines them using the the exposure fusion algorithm described by Mertens *et al.* [9]. This algorithm merges images of multiple illumination levels/exposures by considering the quality measures saturation, contrast, and exposure. A weight can be assigned for each quality measure. The final image is reconstructed by fusing parts from all the images considering the weights given to quality measures, so as to locally improve the quality measures in the final image. Thus, the fused image has better local contrast, exposure, and saturation.

In the reference implementation, equal weight is given to the contrast and exposure parameters in the algorithm. In order to avoid boundary effects due to the abrupt change at finger egdes, the finger image is mirrored along the edges detected during normalization and segmentation.

### 5.2.4 Pattern extraction

The pattern extraction procedure is the maximum curvature method developed by Miura *et al.* [10]. The reference implementation uses the implementation by Ton [14], with a sigma value of 2.5. This stage of the reference implementation is in MATLAB, as opposed to Python, and is run on an external device.

The extracted pattern is then refined by cropping to a smaller region of interest of $450 \times 200$ and performing the following morphological operations to remove noise artefacts and make the extracted pattern uniform.

- Dilation to bridge small gaps in veins.
- Skeletonization to extract structure of the vein pattern.
- Area opening to remove small noise artefacts.
- Dilation to make vein thickness reasonably large relative to image size, so that small shifts do not affect pattern matching.

The pattern thus obtained can be used in a pattern matching algorithm to perform biometric authentication and identification. Progress from a raw vein image to an enhanced image is shown in Figure 2.

## 6. EVALUATION

In order to address **RQ3**, we conducted a preliminary quantitative evaluation. Due to time constraints, the evaluation was informal and limited to 42 finger vein images acquired using the improved pipeline.

## 6.1 Evaluation criteria

The mated and non-mated scores[3] of the old and improved setups, as determined by the maximum curvature [10] algorithm of Miura et al are used to evaluate the performance of the different methods.

It is important to note that the score from the maximum curvature matching method is not a score of confidence, but rather a low-level metric that represents how 'matching' two given vein patterns are. A higher score indicates a good match while a lower score indicates a bad match. The threshold for determining a positive and a negative match has to be experimentally established. This threshold will differ from setup to setup. However, in a good system, the mated scores and non-mated scores will be far apart and clustered together, minimizing the possibility of false acceptance and false rejection.

Thus, the following statistical criteria were devised and used to evaluate the scores.

- Means of mated and non-mated scores: the former should be higher and the latter should be lower.

[3]score of two images of the same finger and two different fingers, respectively.

- Mean of differences between mated and non-mated scores: higher differences are better.
- Standard deviations of mated and non-mated scores: lower is better, since it implies that the scores of each class are clustered together.

## 6.2 Experimental setup

The experiment was set up so as to evaluate the above metrics for

- plain image chosen at same illumination for all fingers such that the image was well-exposed for the most number of fingers,
- old HDR imaging setup by Humblot-Renaux, and
- proposed image setup with Mertens' exposure fusion.

For each setup, the performance of both adaptive illumination and static illumination were evaluated, with four images captured at increasing illumination levels. The multiple images are required for evaluating the HDR and exposure fusion approaches. In the case of adaptive illumination, the illumination was derived from the gray levels 120, 140, 160, and 180. In the case of static illumination the images were obtained at uniform PWM levels of 0.25, 0.50, 0.75, and 1.00.

Images of 42 distinct fingers were captured and used as input data. The dataset was informally gathered and is hence not publicly available. One half of the non-mated scores is of the same finger in the opposite hand of the same person, and the other half is of the same hand of a different person. This was chosen since those non-mated pairs showed the most similarity in shape and size, and hence suitable to evaluate the non-mated scores.

## 6.3 Results

The histograms of the raw scores from each of the experimental setups in Section 6.2 are given in Figure 4. The results of the different statistical metrics outlined in Section 6.1 are given in Table 1. Figure 3 illustrates the difference in image quality with and without adaptive illumination.

While not the primary goal of this research, the pattern enhancement procedure was also evaluated. The raw score histograms for the evaluation of this can be found in Figure 7 (Appendix B).

The average time for the calibration procedure was 2 seconds. The average time for the adaptive illumination adjustment was 20 milliseconds. These processes happened on-device on a Raspberry Pi 3B+. The exposure fusion process took 30 milliseconds on average. This was done on a computer with a 2.7 GHz Intel Core i5 dual core processor.

## 6.4 Discussion

Experimental results and their analysis from our evaluation clearly show that both adaptive illumination as well as the proposed exposure fusion method gives improved results as opposed to static illumination.

The robustness of the adaptive illumination process is clearly visible where the static illumination algorithm fails to provide a well-exposed image for the 6 thin fingers in the dataset, resulting in a blank vein pattern. This can be seen in the bars at 0 in the histograms. Simply using a plain calibrated image alone is seen to make the imaging process robust against such thickness variations, as illustrated by Figure 3. Without adaptive illumination, the finger image

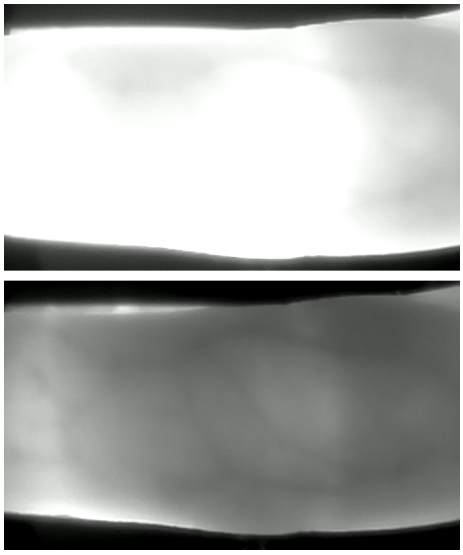

**Figure 3. A thin finger before (top) and after (bottom) application of adaptive illumination.**

is heavily over-exposed. Further, the adaptive illumination algorithm does significantly better in terms of score variations (measured by standard deviation).

In both static and adaptive illumination cases, the proposed exposure fusion process significantly improves image quality and score metrics. Compared to the other approaches, exposure fusion provides scores that are farther apart and more clustered. In the case of static illumination, it manages to produce an image of sufficient quality even in the thin fingers.

From the experiments, it is also evident that a combined adaptive illumination and exposure fusion approach leads to better quality than only one of them. That said, the extent of improvement there is small. However, in the case of the six thin female fingers in the dataset, the combined approach is far superior.

The performance improvement from the combined approach can be explained as follows: the adaptive illumination provides a "best-effort" set of consistent exposures for fusion, and the exposure fusion combines the regions with locally optimal levels of contrast and exposure. If only exposure fusion is used, more images are needed, since of the four images obtained, most of them will either be overexposed (in the case of a thin finger) or underexposed (in the case of a thick finger), leading to a poorer fused image. If only adaptive illumination is used, regions with larger veins will be brighter to compensate for the low average gray level, leading to smaller veins being overexposed, leading to loss of detail. A combined approach mitigates these two issues.

The extra pattern enhancement procedure outlined in Section 5.2.4 also showed a significant improvement in scores of all the methods evaluated. As seen in Figure 7 (Appendix B), applying pattern enhancement moves the two score clusters further apart. This confirms the expectation from visual examination, where it can be seen that additional noise and (false) thickness variations in veins have been reduced.

# 7. RECOMMENDATIONS AND FUTURE WORK

While the research shows promising results, a comprehensive evaluation is needed to establish the statistical signif-

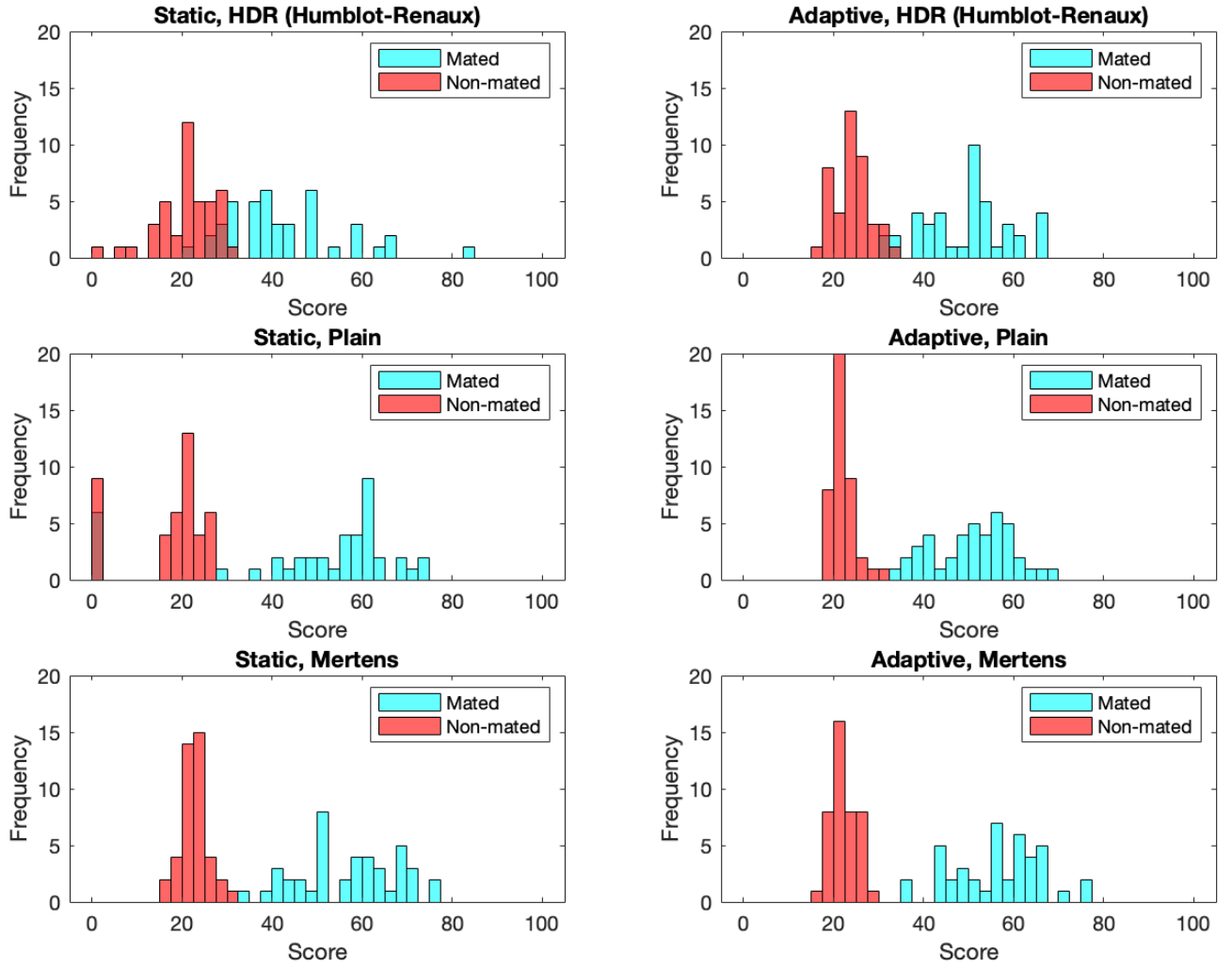


**Figure 4. Histograms of experimental scores. First and second columns contain scores from static and adaptive illumination respectively. The rows are the score of, in order: old HDR imaging approach by Humblot-Renaux, selected plain single image, and proposed new exposure fusion method using the algorithm of Mertens et al.**

| | Static Illumination | | | Adaptive Illumination | | |
|---|---|---|---|---|---|---|
| | Old HDR | Plain Image | New Method | Old HDR | Plain Image | New Method |
| Mean, Mated | 42.51 | 48.32 | 57.11 | 49.31 | 51.09 | 56.49 |
| Mean, Non-mated | 21.02 | 16.91 | 22.67 | 23.99 | 21.90 | 22.39 |
| Mean, Differences | 21.48 | 31.40 | 34.44 | 25.32 | 29.20 | 34.10 |
| Std. Dev., Mated | 13.01 | 22.08 | 10.88 | 9.69 | 8.78 | 9.61 |
| Std. Dev., Non-Mated | 6.44 | 9.30 | 2.87 | 3.87 | 2.67 | 2.86 |

**Table 1. Statistical measures of scores from different setups. Scale from bad to good is colour coded from green to yellow to red, for clarity.**

icance of the improvements.

Only 6 fingers from the set of 42 fingers were female, and it is for those the combined approach made a significant difference. Hence, it is important to explicitly use a diverse set of finger images to evaluate the robustness of the algorithm.

The composed imaging pipeline proposed in the research has several parameters that can be tuned, such as

- the optimal set of gray levels to use in the capture of images using the adaptive illumination,
- the weights of the Mertens exposure fusion algorithm,
- the sigma value used for the vein pattern extraction, etc.

These parameters were determined by trial and error in the research, and may have room for improvement. A more rigorous determination of these need to be done.

In addition to these, it is possible that adaptive illumination calibration alone is sufficient to obtain a good vein image, thereby saving computation and acquisition time. Based on our results, the plain image with adaptive illumination alone does marginally worse than the combined approach with exposure fusion. A more comprehensive study can establish whether this is actually the case.

# 8. CONCLUSION

The research primarily addresses three research questions. The first is regarding finger-adaptive illumination control, for which we present a feedforward finger-adaptive illumination algorithm that is robust to finger variations and operates in constant time. The presented solution is able automatically adjust lighting in a constant time of 200 ms instead of several seconds and effectively makes the image acquisition process robust to finger thickness variations.

Using this illumination algorithm, a multiple exposure fusion approach to finger vein imaging was composed. The devised image pipeline requires minimal manual human intervention or tuning for operation, as opposed to the currently available solutions. The combined solution answers the second research question which requires an alternative to the prior HDR approach, where the alternative also integrates illumination control. The alternative is able to provide better results with only 25% of the previously required number of finger images.

The third research question is to evaluate the combined approach. We evaluated the research work using the mated and non-mated scores and performed a preliminary statistical analysis on them. The developed algorithms were found to improve pattern extraction and matching performance, both separately and in combination. This was reflected by marked decreases in standard deviations of the mated and non-mated score clusters and also increases in the mean difference between them, indicating better separation.

The results of the research provide a practically applicable finger vein imaging pipeline in addition to opening up a potential future areas of research.

# 9. ACKNOWLEDGEMENTS

I would like to extend my sincere gratitude to my supervisor, prof. dr. ir. Raymond Veldhuis, for his valuable advice during the course of this research. I am also grateful to ing. Gert-Jan Laanstra and Koen Rikkerink for the assistance with the imaging device and other friends and acquaintances who volunteered to provide their finger vein images.

# 10. REFERENCES

[1] J. Canny. A computational approach to edge detection. In *Readings in computer vision*, pages 184–203. Elsevier, 1987.

[2] L. Chen, H.-C. Chen, Z. Li, and Y. Wu. A fusion approach based on infrared finger vein transmitting model by using multi-light-intensity imaging. *Human-centric Computing and Information Sciences*, 7(1):35, 2017.

[3] L. Chen, J. Wang, S. Yang, and H. He. A finger vein image-based personal identification system with self-adaptive illuminance control. *Ieee Transactions on Instrumentation and Measurement*, 66(2):294–304, 2016.

[4] P. Debevec and J. Malik. Recovering high dynamic range radiance maps from photographs: Proceedings of the 24th annual conference on computer graphics and interactive techniques. *Los Angeles, USA: SIGGRAPH*, 1997.

[5] G. Humblot-Renaux. Implementation of hdr for image acquisition on a finger vein scanner. July 2018.

[6] A. K. Jain, P. Flynn, and A. A. Ross. *Handbook of Biometrics*. Springer-Verlag, Berlin, Heidelberg, 2007.

[7] P. Jin. Illumination control in sensor of finger vein recognition system. Master's thesis, University of Twente, 2013.

[8] E. C. Lee, H. C. Lee, and K. R. Park. Finger vein recognition using minutia-based alignment and local binary pattern-based feature extraction. *International Journal of Imaging Systems and Technology*, 19(3):179–186, 2009.

[9] T. Mertens, J. Kautz, and F. Van Reeth. Exposure fusion: A simple and practical alternative to high dynamic range photography. In *Computer graphics forum*, volume 28, pages 161–171. Wiley Online Library, 2009.

[10] N. Miura, A. Nagasaka, and T. Miyatake. Extraction of finger-vein patterns using maximum curvature points in image profiles. *IEICE TRANSACTIONS on Information and Systems*, 90(8):1185–1194, 2007.

[11] E. Piciucco, E. Maiorana, and P. Campisi. Palm vein recognition using a high dynamic range approach. *IET Biometrics*, 7(5):439–446, 2018.

[12] S. Rozendal. Redesign of a finger vein scanner.

[13] A. M. Sa, P. C. Carvalho, and L. Velho. High dynamic range image reconstruction. *Synthesis Lectures on Computer Graphics and Animation*, 2(1):1–54, 2008.

[14] B. Ton. Vascular pattern of the finger: Biometric of the future? Master's thesis, University of Twente, 2012.

[15] B. T. Ton and R. N. Veldhuis. A high quality finger vascular pattern dataset collected using a custom designed capturing device. In *2013 International Conference on Biometrics (ICB)*, pages 1–5. IEEE, 2013.

[16] E. Vissers. Acquisition time and image quality improvement by using hdr imaging for finger-vein image acquisition. page 6.

# APPENDIX

## A. ILLUMINATION REGRESSION ALGORITHM

**Algorithm 1** Illumination regression algorithm

**procedure** REGRESSION($\mathbf{L}, \mathbf{c}, iterations$)
  $\mathbf{s} \leftarrow$ column_sum($\mathbf{L}$)
  $\mathbf{L}' \leftarrow$ column_normalise($\mathbf{L}$)
  $\mathbf{L}'' \leftarrow \mathbf{L}'$
  **for all** $i \in [0, \text{row\_count}(\mathbf{L}) \wedge i \in \mathbf{Z})$ **do**
    $\mathbf{L}''_{i*} \leftarrow \mathbf{L}''_{i*} * \max(\mathbf{L}_{i*})/\max(\mathbf{L})$
  **end for**
  $\mathbf{W} \leftarrow$ transpose($\mathbf{L}''$)
  $count \leftarrow 0$
  **while** $count < iterations$ **do**
    $\mathbf{v} \leftarrow \mathbf{p} * \mathbf{L}$
    $\mathbf{e} \leftarrow \mathbf{v} - \mathbf{c}$
    $\mathbf{e} \leftarrow \mathbf{e}/\mathbf{s}$
    $\mathbf{d} \leftarrow \mathbf{e} * \mathbf{W}$
    $\mathbf{p} = \mathbf{p} - \mathbf{d}$
  **end while**
  **return p**
**end procedure**

## B. ADDITIONAL FIGURES

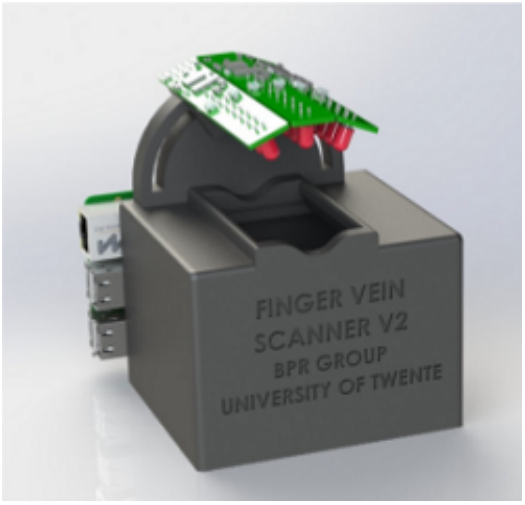


**Figure 5. The scanning device.**

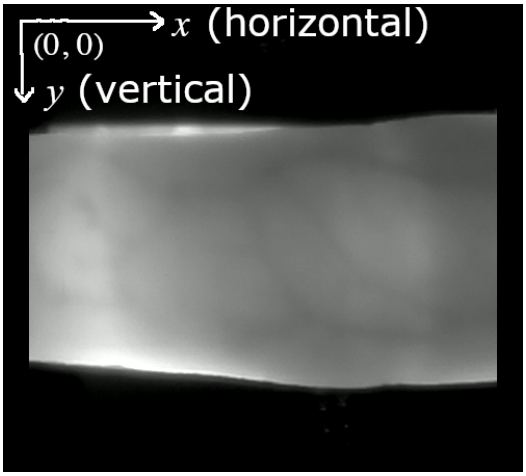


**Figure 6. Coordinate system and directions used in model.**

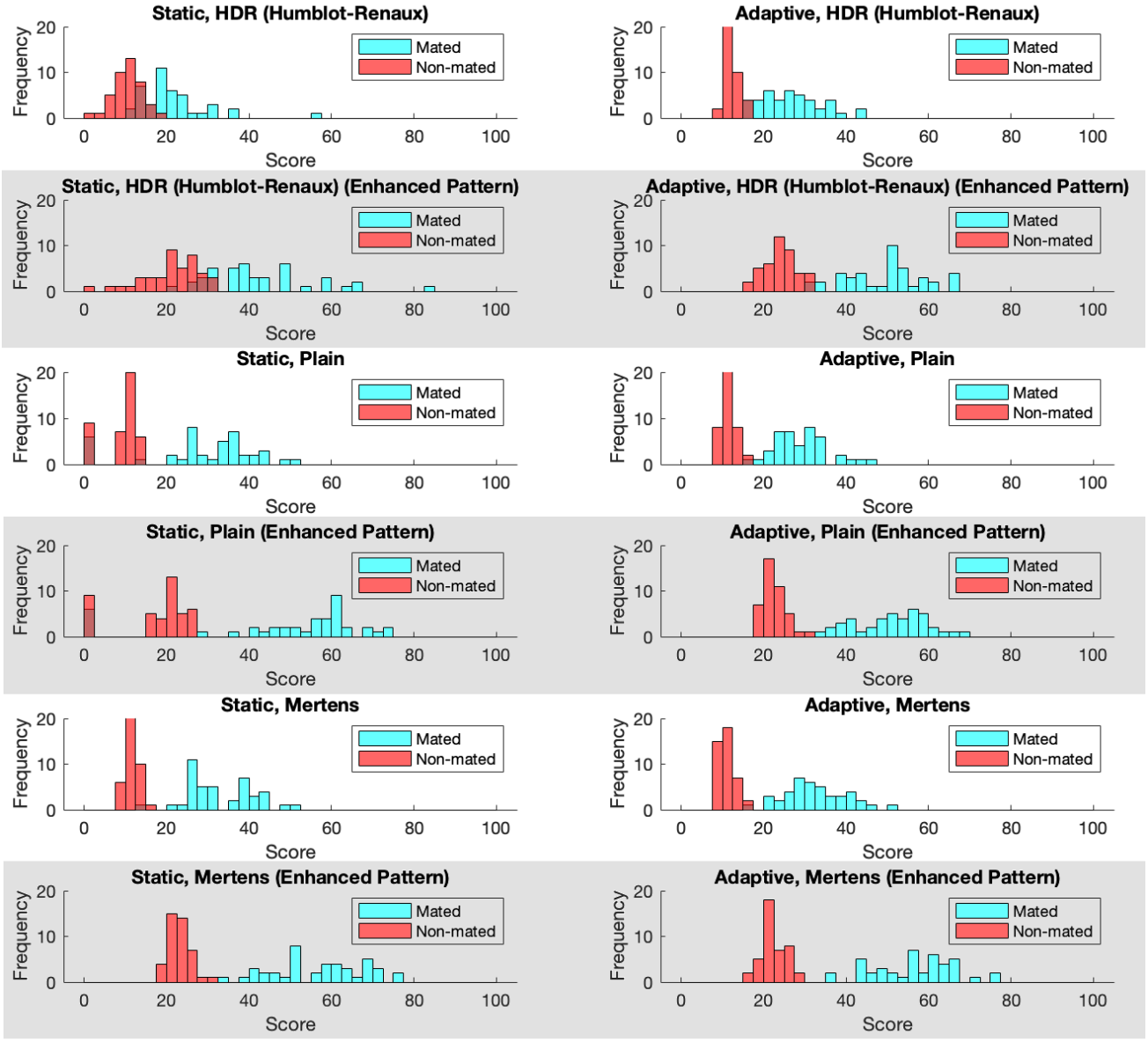


**Figure 7. Histograms of experimental scores. First and second columns contain scores from static and adaptive illumination respectively. The rows are the scores of, in order: old HDR imaging approach by Humblot-Renaux, old HDR imaging approach by Humblot-Renaux with pattern enhancement, selected plain single image, selected plain single image with pattern enhancement, proposed new exposure fusion method using the algorithm of Mertens *et al.*, proposed new exposure fusion method using the algorithm of Mertens *et al.* with pattern enhancement. The grey rows have scores of the methods immediately above them, but with pattern enhancement.**